An extracellular cell-attached pullulanase confers branched -glucan utilization in human gut Lactobacillus acidophilus

Møller, Marie Sofie; Goh, Yong Jun; Rasmussen, Kasper Bøwig; Cypryk, Wojciech; Celebioglu, Hasan Ufuk; Klaenhammer, Todd R; Svensson, Birte; Abou Hachem, Maher

Published in:
Applied and Environmental Microbiology

Link to article, DOI:
10.1128/AEM.00402-17

Publication date:
2017

Document Version
Peer reviewed version

An extracellular cell-attached pullulanase confers branched α-glucan utilization in human gut *Lactobacillus acidophilus*

Marie S. Møller,[a] Yong Jun Goh,[b] Kasper Bøwig Rasmussen,[a] Wojciech Cypryk,[a] Hasan Ufuk Celebioglu,[a] Todd R. Klaenhammer,[b] Birte Svensson,[a] Maher Abou Hachem[a]#

Department of Biotechnology and Biomedicine, Technical University of Denmark, Kgs. Lyngby, Denmark[a]; Department of Food, Bioprocessing and Nutrition Sciences, North Carolina State University, 7 Raleigh, North Carolina[b]

Running Head: Metabolism of branched α-glucans by *L. acidophilus*

#Address correspondence to Maher Abou Hachem, maha@bio.dtu.dk or Yong Jun Goh, yjgoh@ncsu.edu.

ABSTRACT

Of the few predicted extracellular glycan-active enzymes, glycoside hydrolase family 13 subfamily 14 (GH13_14) pullulanases are the most common in human gut lactobacilli. These enzymes share a unique modular organization, not observed in other bacteria, featuring a catalytic module, two starch binding modules, a domain of unknown function, and a C-terminal surface layer association protein (SLAP) domain. Here we explore the specificity of a representative of this group of pullulanases, *La*Pul13_14 and its role in branched α-glucans metabolism in the well characterized *Lactobacillus acidophilus* NCFM that is widely used as a probiotic. Growth experiments of *L. acidophilus* NCFM on starch-derived branched substrates revealed preference for α-glucans with short branches of about two to three glucosyl moieties over amylopectin with longer branches. Cell-attached debranching activity was measurable in the presence of α-glucans but was repressed by glucose. The debranching activity is conferred exclusively by *La*Pul13_14 and is abolished in a mutant strain lacking a functional *La*Pul13_14 gene. Hydrolysis kinetics of recombinant *La*Pul13_14 confirmed the preference for short branched α-glucan oligomers consistent with the growth data. Curiously, this enzyme displayed the highest catalytic efficiency and the lowest K_m reported for a pullulanase. Inhibition kinetics revealed mixed inhibition by β-cyclodextrin suggesting the presence of additional glucan binding sites besides the active site of the enzyme, which may contribute to the unprecedented substrate affinity. The enzyme also displays high thermostability and higher activity in the acidic pH range reflecting adaptation to the physiologically challenging conditions in the human gut.

IMPORTANCE

Starch is one of the most abundant glycans in human diet. Branched α-1,6-glucans in dietary starch and glycogen are non-degradable by human enzymes and constitute a metabolic resource for the gut microbiota. The role of health-beneficial lactobacilli prevalent in the human small intestine in starch metabolism remains unexplored in contrast to colonic bacterial residents.

This study highlights the pivotal role of debranching enzymes in the break-down of starchy branched α-glucan oligomers (α-limit dextrins) by human gut lactobacilli exemplified by *Lactobacillus acidophilus* NCFM, which is one of the best characterized strains used as probiotics.

Our data bring novel insight into the metabolic preference of *L. acidophilus* for α-glucans with short α-1,6-branches. The unprecedented affinity of the debranching enzyme that confers growth on these substrates reflects its adaptation to the nutrient-competitive gut ecological niche and constitutes a potential advantage in cross-feeding from human and bacterial dietary starch metabolism.

INTRODUCTION

The human gastrointestinal tract is inhabited by a vast, diverse and dynamic microbial community (1), which is shaped by competition amongst the different taxa and selection by the host. *Firmicutes* and *Bacteroidetes* are the prevalent bacterial phyla of the human gut microbiota (HGM), followed by *Actinobacteria*, *Proteobacteria* and *Verrucomicrobia* in healthy adults (2). This microbial community provides protection against enteric pathogens and endows the host with metabolic activities that are not encoded in the human genome. More importantly, the interplay between diet and the HGM is currently recognized as a major effector of the composition of this community (2, 3) and as a negotiator of human metabolism (4, 5). A key feature of the HGM is the ability to harvest energy from both host-derived and dietary glucans, particularly those resistant to digestion by human enzymes (6). Consequently differential glycan metabolism is a key affecter of the microbiota composition (7).

Starch is the most abundant glycan in human diet. This polysaccharide is a composite of two α-glucans: the linear α-1,4-glucan amylose, and amylopectin, which possesses approximately 5% α-1,6-branch points with average branch lengths of 18–25 glucosyl moieties (8). Starch occurs naturally as supramolecular insoluble granules with semi-crystalline regions (8). These granules differ in size, structural properties as well as digestibility by bacterial and human enzymes. Humans digestive enzymes mainly target the α-1,4-glucosidic bonds, but are less efficient in hydrolyzing α-1,6-branches in starch (9). The digestibility of starch varies considerably based on botanical origin, crystal-packing and processing (10). Significant amounts of dietary starch escape digestion in the upper gastrointestinal tract (resistant starch, RS) (11) and are fermented in the colon by members of the gut microbiota (12–15). The small intestine, however, is dominated by bacteria from the Gram-positive *Lactobacillaceae* and the Gram-negative *Enterobacteriaceae* families (16). The former family contains human gut adapted lactobacilli from the *L. acidophilus* group, many strains of which are used as probiotics (17).

The ability of health beneficial bacteria from the *Lactobacillus* genus to grow on starch is limited to a handful of strains that grow on the soluble, but not granular starch (18, 19). Growth on short starch-derived malto-oligosaccharides (α-gluco-oligosaccharides), however, is well established within this genus. Interestingly, a RS-rich diet appeared to boost the numbers of lactobacilli and lactate production in the distal colon in rodent models (20, 21). A recent human study in rural Malawi children showed a similar increase in lactobacilli after RS intake (22). A possible explanation of these observations is cross-feeding on short α-glucans that are produced by primary starch degraders (14, 23). Cross-feeding requires efficient capture and transport systems and intracellular degrading enzymes reported to be conserved in this genus (24). The intracellular α-glucoside utilization machinery of acidophilus group lactobacilli (17) is relatively well understood (24–26). By contrast, the extracellular α-glucanolytic capabilities within this group of bacteria associated with a healthy gut microbiota are currently unexplored.

The commercial strain *Lactobacillus acidophilus* NCFM, which is used as probiotic, is among the best-studied of this taxonomic group (17). The genome of *L. acidophilus* NCFM (27) encodes nine enzymes of glycoside hydrolase family 13 (GH13), which harbors α-glucan active enzymes according to the CAZy database (28). The only predicted α-glucan active extracellular enzyme, however, is a pullulanase-type α-glucan debranching enzyme. This enzyme is multi-modular comprising an N-terminal starch binding domain of carbohydrate binding module family 41 (CBM41), followed by a domain of unknown function, a CBM48 domain, a GH13 subfamily 14 (GH13_14) catalytic module (28) and a C-terminal surface layer association protein (SLAP) (28, 29) (Fig. 1). Pullulanases catalyze hydrolysis of α-1,6-linked branches in glycogen, amylopectin and other starch derived glucans, as well as pullulan (Fig. 2) (30–32).

In this study, we show that extracellular cell-attached pullulanase activity can be measured upon growth of *L. acidophilus* NCFM on a range of oligomeric and polymeric α-glucans, whereas this activity is repressed upon growth on glucose. We also establish the exclusive role of the debranching enzyme *La*Pul13_14 in the degradation of branched α-glucans in this bacterium. The

100 catalytic and binding properties of the recombinant *La*Pul13_14 were investigated showing
101 unprecedented substrate affinity and a clear preference towards short-branched α-glucan oligomers
102 as compared to amylopectin. These findings are consistent with the growth profile of *L. acidophilus*
103 NCFM. Together, these findings highlight the role of *La*Pul13_14 and its homologues in mediating
104 the utilization of branched oligomers derived from starch degradation in the human gut.
105
106 **MATERIALS AND METHODS**
107 **Materials.** High-purity (>95%) chemicals and commercial enzymes were from Sigma-Aldrich,
108 MO, USA, unless otherwise stated. Pullulan (>95%) and β-limit dextrin (>97%) were from
109 Megazyme (Bray, Ireland). The maltotetraose used for the growth/induction experiment was an in-
110 house preparation (purity >92%; impurity was maltotriose). The branched α-limit dextrin used for
111 the kinetic analysis (kind gift from the late Bent S. Enevoldsen) comprises a mixture of two
112 isomers: 6^2-α-D-maltosyl-maltotriose and α-D-glucosyl-maltotetraose.
113 **Bioinformatics analysis**. Sequences of *La*Pul13_14 homologues were extracted from the
114 Carbohydrate-Active Enzymes database (CAZy; www.cazy.org) (28) using the CAZy tools
115 provided by Alexander Holm Viborg (http://research.ahv.dk). Domain organisation of the protein
116 sequences was analysed using a combination of batch searches in the Conserved Domain Database
117 (29) and search in the Pfam protein families database (33). Identification of putative extracellular
118 enzymes was done based on predictions from the SignalP 4.1 Server (34).
119 **Growth experiments**. *L. acidophilus* NCFM was grown on glucose, maltose, maltotriose,
120 maltotetraose, a mixture of glucose and maltose (1:1 based on weight), β-limit dextrin,
121 amylopectinor pullulan. Growth was performed in 14 ml semi-defined medium (SDM) (35) with
122 0.5% (w/v) carbohydrate in 15 ml conical culture tubes, which were inoculated with an overnight
123 culture previously grown on SDM supplemented with 1% (w/v) glucose to an optical density at 600
124 nm (OD_{600}) of 0.1 (0.04 as measured on 200 µl culture in a 96-well plate using a microplate reader).
125 The cultures were incubated at 37°C and 200 µl samples were withdrawn every 1–2 hours for OD_{600}

measurements. When the cultures reached late log-phase (after approx. 10 h), 2 × 1 ml samples per culture were collected and spun down (20,000 × *g*, 10 min, 4°C) and the cells and supernatant were assayed for enzymatic acitivity (see below). The growth experiments of the *La*Pul13_14 deletion mutant (ΔLBA1710, see below) were performed in a similar manner on glucose and maltose and all growth experiments were performed in duplicates. The supernatants from the growth experiments were assayed for pullulanase activity using the standard reducing sugar assay described below, whereas the cells were washed twice with 0.9% NaCl before measurements of pullulanase activity (described below).

Additional growth experiments were performed to compare the growth of *L. acidophilus* NCFM to *L. acidophilus* DSM-20242, which possesses identical organization of the maltodextrin utilization cluster as *L. acidophilus* NCFM and is used as a control, and *L. acidophilus* DSM-9126, which possesses a typical maltrodextrin utilization locus and lacks the inserted transposase present in both *L. acidophilus* NCFM and DSM-20242. Anaerobically grown cultures in MRS were transferred once in SDM with1% glucose (anaerobic), and the resulting cultures were used to inoculate (1% or equivalent cell density for weaker-growing strains) the SDM-based growth media (0.5% carbohydrate source, 200 µL per well, in duplicate wells and conditions). Growth was monitored with a microtiter plate reader for 60 h.

Maltooligosaccharide uptake. *L. acidophilus* NCFM was grown on a total of 0.5% (w/v) mixture of maltose, maltotriose, and maltotetraose (1:1:1 based on weight) as described above. Samples were collected during growth for OD_{600} measurements and oligosaccharide analysis, which was performed as follows: 1 ml sample was spun down (20,000 × *g*, 10 min, 4°C), 80 µl supernatant was diluted 100-fold in 0.1 M NaOH and sterile filtered through pre-rinsed (with milliQ) 30 kDa filters (Amicon Ultra spin filters; Millipore, MA, USA) before the content of maltose, maltotriose and maltotetraose was analysed using high performance anion exchange chromatography with pulsed amperometric detection (HPAEC-PAD) using an ICS3000 system, equipped with CarboPac PA200 anion exchange column (Dionex Corporation, Sunnyvale, CA)

using a 2-step sodium acetate gradient (0–7 min: 37.5–75 mM and 7–30 min: 75–300 mM) and a constant concentration of 0.1 M NaOH at 25°C at 0.35 ml min^{-1}. After each run the column was regenerated with a constant concentration of 0.1 M NaOH and 400 mM sodium acetate for 5 min, followed by a gradient from 400 mM to 37.5 mM sodium acetate over 5 min, and finally an equilibration with 37.5 mM sodium acetate and 0.1 M NaOH for 5 min.

Construction of LBA1710 (*La*Pul13_14) deletion mutant. The 3,555-bp *lba1710* gene encoding the *La*Pul13_14 in *L. acidophilus* NCFM was deleted using a *upp*-based counterselective gene replacement system (36). Briefly, a 3,489-bp in-frame deletion (98% of gene) within *lba1710* was constructed by first PCR-amplifying the 629-bp and 646-bp DNA segments flanking the upstream and downstream of the *lba1710* deletion target, respectively, using primer pairs 1710-1/1710-2 (5'-GTAATAGGATCCACAACAAGCTCAAGGGATTCA-3' / 5'-AACACCTTTTGTTCCCCA-3') and 1710-3/1710-4 (5'-TGGGGAACAAAAGGTGTTGCAGTGAATGTTGTTATTGAAG-3' / 5'-TTAGTAGAATTCCTTGAGGGAGCTCAACTTTC-3') (restriction sites were underlined), with PfuUltraII HS DNA Polymerase (Agilent Technologies, California, USA). Both purified PCR products were fused and amplified to generate copies of Δ*lba1710* allele via splicing by overlap extension PCR (SOE-PCR) (37), using 10 ng of each PCR product as amplification templates in a 50-µL PCR reaction with primer pair 1710-1/1710-4 (see above). Purified SOE-PCR products (1,275 bp) were digested with BamHI and EcoRI and ligated into compatible ends of pTRK935 counterselectable integration vector. Construction of the resulting recombinant integration plasmid containing the Δ*lba1710* allele, designated pTRK1085, and the recovery of plasmid-free double recombinants with 5-fluorouracil were performed as described previously (36, 38). Double recombinants with Δ*lba1710* allele were screened by colony PCR using primer pair 1710-1/1710-4. In-frame deletion and sequence integrity were confirmed by PCR and DNA sequencing using primer pair 1710-5/1710-6 (5'-TGAGCAAGTTAGCGCATCTG-3' / 5'-GCTGGTGTTGCAGAAGTAG-3'), which specifically anneal to the flanking region of the

178 *lba1710* gene. One of the confirmed Δ*lba1710* deletion mutants, designated as NCK2325, was
179 selected for further studies.

180 **Production and purification of recombinant *La*Pul13_14**. *L. acidophilus* NCFM genomic
181 DNA, prepared as previously described (26), was used to amplify the *La*Pul13_14 gene (locus tag
182 number: LBA1710; GenBank accession number AAV43522.1), with the sense primer (5'-
183 CTAGCTAGCGCAGAAACACCAGATGCTGG-3') and the antisense primer (5'-
184 CCGCTCGAGAGCTTTTACTTCAATAACAACATTC-3') (restriction sites were underlined).
185 The PCR amplicon encoding the mature peptide (3,468 bp) lacking the signal peptide (bp 1−105,
186 corresponding to amino acid residues 1–35, see Fig. 1) was cloned within the NheI and XhoI
187 restriction sites in pET21a(+) (Novagen, Darmstadt, Germany) and transformed into *Escherichia*
188 *coli* XL10-Gold Ultra-competent cells (Stratagene, California, US) following the manufacturer's
189 protocols. Transformants harboring pET21a(+)-*La*Pul13_14, were selected on LB-agar plates with
190 100 µg ml^{-1} ampicillin and verified by restriction analysis and full sequencing. *E. coli* Rosetta
191 (DE3) cells (Invitrogen, USA) transformed with pET21a(+)-*La*Pul13_14 were used for production
192 of the enzyme.

193 The enzyme was produced in a 5-liter bioreactor (Biostat B Plus, Sartorius Stedium, Germany) as
194 described elsewhere (39) with the following modifications: 3.7 liter defined medium was inoculated
195 to OD_{600}=1.5 with an overnight culture grown in LB medium. The fermentation was carried out at
196 37°C until OD_{600}=8, before lowering the temperature to 15°C and induction of expression using 100
197 µM isopropyl-β-D-thiogalactopyranoside. Cells were harvested (6,000 × *g*, 20 min, 4°C) at
198 OD_{600}=30.5 after 67 h of induction. The cell pellet was resuspended in buffer A (10 mM HEPES pH
199 7.4, 25 mM imidazole, 40% glycerol, 0.5 M NaCl, 1 mM $CaCl_2$, 0.005 % (v/v) Triton X-100) and
200 disrupted by high-pressure homogenization at 1000 bar. Disintegrated cells were treated with
201 benzonase nuclease (Invitrogen; 30 min at room temperature) and centrifuged twice (40,000 × *g*, 30
202 min, 4°C). The supernatant was filtered (0.45 µm) and loaded onto a 5 ml HisTrap HP column (GE
203 Healthcare, Uppsala, Sweden). After washing with 10 column volumes buffer A including 26 mM

imidazole, bound protein was eluted with a linear gradient from 3–80% buffer B (10 mM HEPES pH 7.4, 400 mM imidazole, 40% glycerol, 0.5 M NaCl, 1 mM $CaCl_2$). Fractions containing protein were pooled and concentrated (30 kDa Amicon Ultra spin filters; Millipore) to 5 ml and loaded onto a pre-equilibrated HiLoad 26/60 Superdex G200 column (GE Healthcare) and eluted with 50 mM MES, pH 6.0, 1 mM $CaCl_2$, 20% glycerol, 150 mM NaCl at 0.75 ml min^{-1}. Fractions containing *La*Pul13_14 were pooled and desalted on a HiPrep 26/10 Desalting column (GE Healthcare) against 1 mM HEPES, pH 7.0. Desalted protein fractions were pooled and loaded onto a Resource Q column (6 ml; GE Healthcare) equilibrated with 10 mM HEPES, pH 7.0, at a flow rate of 2 ml min^{-1}. Protein was eluted by a linear gradient (from 0–100% in 30 column volumes) of 10 mM HEPES, pH 7.0, 0.5 M NaCl. Fractions containing *La*Pul13_14 were pooled, concentrated, and buffer exchanged (30 kD Amicon Ultra spin filters, Millipore) to 50 mM MES pH 6.0, 20% glycerol, 0.5 mM $CaCl_2$, 150 mM NaCl. The concentration of *La*Pul13_14 (SDS-PAGE) was determined spectrophotometrically using a molar extinction coefficient ε_{280}=179,566 $M^{-1}cm^{-1}$ as determined by amino acid analysis (40).

Enzyme activity assays and kinetics. Determination of specific activity as well as kinetic parameters of *La*Pul13_14 was performed using a reducing sugar assay as previously described (41). In short; 1.1 ml reactions containing substrate (0.225 mg ml^{-1} pullulan for specific activity; 0.02–1 mg ml^{-1} pullulan, 0.1–10 mg ml^{-1} potato amylopectin dissolved in 8 % (v/v) DMSO or 0.225–9 mg ml^{-1} β-limit dextrin for kinetic analysis) and *La*Pul13_14 (0.05–1.5 nM) in assay buffer (20 mM sodium acetate pH 5.0, 5 mM $CaCl_2$, 0.005% TritonX-100) were incubated at 37 ˚C and aliquots (200 µl for pullulan, and 100 µl for amylopectin and β-limit dextrin) were removed at five time points (3, 6, 9, 12, and 15 min) and added to 500 µl stop solutions (0.4 M sodium carbonate pH 10.7, 2.5 mM $CuSO_2$, 2.5 mM 4,4'-dicarboxy-1,2'-biquinoline, 6 mM L-serine). Milli-Q water was added to a final volume of 1 ml and A_{540nm} was measured after 30 min incubation at 80°C. The release of reducing sugars was quantified using a maltose standard. One activity unit (U) is defined as the amount of enzyme that releases one micromole of maltose reducing-sugar equivalents per

min from pullulan under assay conditions. The kinetic parameters K_m and k_{cat}, were determined by fitting the Michaelis-Menten equation to the initial velocity data. The data obtained were analyzed using the Enzyme Kinetics Module 1.0 of the program Sigmaplot 9.01 (Systat Software, Chicago, IL). Inhibition kinetics of *La*Pul13_14 by β-cyclodextrin (β-CD) were investigated using pullulan as substrate. The kinetics assay was done as described above, but with 50 µM β-CD included. The data obtained was analyzed by fitting competitive, non-competitive, mixed inhibition models to the data using the Enzyme Kinetics Module 1.0 of the program Sigmaplot 9.01 (Systat Software, Chicago, IL), and the inhibition kinetics models were ranked based on χ^2 of the fits.

The hydrolysis kinetics parameters of the branched α-limit dextrin mixture described above (five glucose units, maltosyl branch) by *La*Pul13_14 were determined using HPAEC-PAD. The starting reaction volume was 300 µl including branched substrate (0.0625–1 mM) and 0.53 nM *La*Pul13_14 in 20 mM sodium acetate pH 5.0, 5 mM $CaCl_2$, 0.005% (v/v) TritonX-100. At four time points (3, 6, 9, and 12 min) 60 µl aliquots were drawn and mixed with 15 µl 0.5 M NaOH. The samples were spun (20,000 × *g*, 5 min, 4°C) before 65 µl samples were mixed with 65 µl 0.1 M NaOH. The products were quantified based on peak areas from HPAEC-PAD analysis, which was performed as described above.

The described standard reducing sugar assay was also used to determine the pullulanase activity in the *L. acidophilus* culture supernatant and in the washed cell pellets, with the following exceptions: cells from 1 ml culture in the late log phase (see above) were resuspended in 600 µl preheated (37ºC) pullulan solution (0.4 mg ml^{-1} pullulan, 40 mM sodium acetate pH 5.0, 0.5 mM $CaCl_2$, 0.005% (v/v) Triton X-100), while 100 ul culture supernatant was mixed with 500 µl 0.48 mg ml^{-1} pullulan solution. Aliquots (100 µl) were drawn after 0, 1, 2, and 3 h. The samples were spun down at 4°C for 2 min, and 75 µl cell free sample was mixed with 500 µl stop solution (0.4 M sodium carbonate pH 10.7, 2.5 mM $CuSO_2$, 2.5 mM 4,4'-dicarboxy-1,2'-biquinoline, 6 mM L-serine) and 425 µl milliQ water. As a control, the degradation products from the assay with whole cells and pullulan were analyzed using thin layer chromatography (TLC). Samples (6 µl) were

drawn after 0 and 19 h of reaction and spotted directly onto a TLC Silica 60 F_{254} plate (Merck, Darmstadt, Germany), developed by isopropanol/ethyl acetate/water (60:20:20, v/v) and sprayed with 2% (w/v) orcinol in ethanol/H_2SO_4/water (80:10:10) followed by tarring at 300ºC. The following standards were included on the gel (1 µl): 20 mM of either glucose, maltose, maltotriose and panose in water.

Temperature and pH activity profiles. The reducing sugar assay described above was used for determining the dependence of initial reaction rates on temperature in the range 7−80°C using 0.46 nM *LaPul13_14* and 0.225 mg ml^{-1} pullulan. The dependence of activity on pH in the range 2.0–8.5 was assayed using the reducing sugar assay described above in 20 mM of either glycine (pH 2.0–3.5), sodium acetate (pH 3.5–5.5), MES (pH 5.5–7.0), or HEPES (7.0–8.5) all including 0.5 mM $CaCl_2$ and 0.005% bovine serum albumin.

Surface plasmon resonance (SPR) binding analysis of cyclodextrins. The affinity of *La*Pul13_14 towards α-, β-, and γ-CD was analyzed using SPR on a BIAcore T100 (GE Healthcare). Random amine coupling was used to immobilize the enzyme on a CM5 sensor according to the manufacturer's protocol using 100 µg ml^{-1} protein in 10 mM sodium acetate, pH 4, 0.5 mM $CaCl_2$, and 1 mM β-CD to a final chip density of 5477 response units (RU). The analysis comprised 100 s and 90 s for the association and dissociation phases, respectively, at a flow rate of 30 µl min^{-1} and 25ºC at 19 β-CD concentrations (0.25–1024 µM) as well as 18 α-CD and γ-CD concentrations (3–5000 µM) all in 10 mM sodium acetate, pH 5.0, 150 mM NaCl, 0.005% (v/v) P20 surfactant. In the case of β-CD the interaction was analysed at 15ºC and 37ºC in addition to the 25ºC standard analysis. Furthermore, the interaction with β-CD was also analyzed at pH 7.0 in 10 mM HEPES, pH 7.0, 150 mM NaCl, 0.005% P20 surfactant. A one site binding model was fit to the steady-state response blank and reference cell corrected sensorgrams using the BIA evaluation software supplied with the instrument.

Starch binding assay. Barley starch was washed three times in water followed by one time in assay buffer (40 mM sodium acetate pH 5.0, 0.5 mM $CaCl_2$, 0.005% (v/v) Triton X-100) overnight.

Fifty microliters of *La*Pul13_14 diluted to 40 nM in assay buffer and 450 µl of washed starch suspension in reaction buffer (25, 50, 100, 200 mg ml^{-1}) were mixed and shaken vigorously at 4°C for 30 min. The mixture was subsequently centrifuged (20,000 × *g*, 5 min, 4°C) and 110 µl of supernatant were used for the standard reducing sugar assay described above using 0.72 mg ml^{-1} pullulan in assay buffer as substrate. Samples were withdrawn at 0 and 10 min and directly transferred to stop solution and the standard assay protocol was followed. The fraction of enzyme bound to starch was determined based on the activity in the supernatant relative to an enzyme sample without starch included.

RESULTS

***L. acidophilus* growth on α-glucans and extracellular pullulanase activity.** To assess the α-glucan metabolic capabilities of *L. acidophilus* NCFM, growth was performed on glucose, α-1,4-linked maltooligosaccharides with degree of polymerization (DP) of 2−4, amylopectin, β-limit dextrin possessing short branches (degradation product from hydrolysis of amylopectin by β-amylase) and pullulan (Fig. 2). *L. acidophilus* NCFM clearly preferred glucose followed by maltose, whereas the growth on the larger malto-oligosaccharides was much weaker (Fig. 3A). Amongst the branched polymeric α-glucans, only β-limit dextrin with the short branches (mainly maltosyl) seemed to sustain clear, albeit low, growth (Fig. 3A), whereas no significant growth was observed on pullulan and amylopectin (data not shown). Cells harvested in the late log phase displayed highest cell-associated pullulanase activity when maltose was used as a carbon source, but maltotriose, maltotetraose and β-limit dextrin also resulted in a significant pullulanase activity (Fig. 3B). By contrast no significant activity was detected when the cells were grown on either glucose or a glucose:maltose 1:1 mixture. No pullulanase activity was detected in the culture supernatant, *i.e*. all pullulanase activity measured is entirely associated with the cells.

The uptake preference of maltooligosaccharides with degree of polymerization 2–4 by *L. acidophilus* NCFM was analyzed using a mixture of maltose, maltotriose, and maltotetraose as

carbohydrate source and the depletion of these saccharides in culture supernatants was monitored. Maltose was clearly the preferred substrate, but both maltotriose and maltotetraose were also taken up, albeit at a considerably slower rate (Fig. 3C).

To verify that the measured cell-associated pullulan hydrolyzing activity stems from *La*Pul13_14, the gene encoding this enzyme was deleted and the *L. acidophilus* NCFM gene KO strain was grown on glucose or maltose. No cell-associated pullulanase activity was measured from this strain, although the growth rate on maltose was much higher as compared with wildtype (Fig. 4).

Enzymatic properties of *La*Pul13_14. *La*Pul13_14 was produced recombinantly in *E. coli* and purified (yield 0.26 mg g^{-1} cell wet weight) and migrated according to the predicted molecular mass of 129.4 kDa. The enzyme displayed a very high specific activity of 611 U mg^{-1} toward pullulan corroborating the predicted specificity. The highest specific activity was measured at pH 5.0, and the enzyme retained more than 50% of its maximum activity in the pH range 2.5−6.5. The highest activity was measured at 55°C (at pH 5.0) and the Arrhenius activation energy was determined to 60.2 kJ mol^{-1}.

Kinetic analysis. The kinetic analysis performed on pullulan showed an exceptionally high catalytic efficiency (k_{cat}/K_m) of 10368 ml $s^{-1}mg^{-1}$ owing to a combination of a very low K_m value (0.05 mg ml^{-1}) and a high catalytic turnover number (k_{cat}, 518 s^{-1}) (T). Among the branched substrates tested, the catalytic efficiency decreased with increasing substrate size and branch length. Thus, the catalytic efficiency on the branched substrate β-limit dextrin, which has mainly maltosyl branches, was 14-fold higher than the corresponding value on amylopectin.

Cyclodextrins are well-known starch mimic molecules that bind tightly in the active sites of pullulanases resulting in apparent competitive inhibition (41). Interaction of α-, β-, and γ-CD with *La*Pul13_14 was determined by SPR analysis. β- and γ-CD had dissociation constants (K_D) of 10.8 and 11.2 μM, respectively (

TABLE **1**. Binding of cyclodextrins to *La*Pul13_14 determined by surface plasmon resonance.

). Interestingly, enzymatic inhibition kinetics analysis with pullulan revealed that the inhibition of *La*Pul13_14 with β-CD was not pure competitive inhibition, but was mixed type inhibition giving a K_i of 35.9 µM. This is an average value of the binding to the active site and possibly other binding site of lower affinity. The analysis of the binding of the enzyme to granular starch revealed only very low binding affinity hampering a reliable quantitative measurement (Fig. S1).

DISCUSSION

***Surface layer association proteins mediate attachment of glycan active enzymes and other functionally important enzymes to the cell envelope in* Lactobacillus.** *L. acidophilus* NCFM is one of the most well-studied gut bacteria, which is ascribed health benefits and used as a commercial probiotic (42–45). The commercial and physiological relevance of *L. acidophilus* NCFM has spurred wide interest in the saccharide uptake and catabolism machinery of this organism to identify efficiently utilized glycans with potential as prebiotics (25, 46, 47). A few intracellular carbohydrate active enzymes (CAZymes) from *L. acidophilus* NCFM have been characterized including those active on maltose (26) and α-1,6-linked isomaltooligosaccharides (24). However, insight is scarce into the extracellular CAZymes encoded by this bacterium and related human gut adapted lactobacilli (27). Recently, the first extracellular glycoside hydrolase from *L. acidophilus* NCFM was shown to be a β-*N*-acetylglucosaminidase autolysin essential for cell division (48). This enzyme harbors a surface layer association protein (SLAP) domain (Pfam family PF03217 (33)) that confers noncovalent attachment to the proteinaceous outermost surface layer common in several lactobacilli (49). SLAP domains also occur at the C-termini of other functionally important proteins such as autolysins, fibronectin and mucin binding proteins, putative peptidases, nucleases, glycoside hydrolases as well as polysaccharides lyases according to the Pfam database (33). This suggests that SLAP domains constitute a general cell attachment scaffold that is fused to a select set

of activities destined for cell-surface display. The prevalence of this domain in the S-layer exoproteome of distinct lactobacilli is also in agreement with this role (50).

In this study, we present the functional characterisation of the SLAP domain-containing enzyme from *L. acidophilus* NCFM that is active on starch derived dietary glucans.

La*Pul13_14 is a cell-attached debranching enzyme that exclusively confers the utilization of branched α-glucans in* L. acidophilus. Growth experiments of *L. acidophilus* NCFM clearly showed a preference for glucose and maltose as substrates. Low levels of growth was observed on the longer α-1,4-maltooligosaccharides maltotriose and maltotetraose, and on β-limit dextrin, which is a model susbtrate that contains only short α-1,6-branches (shown experimentally to be main 2–3 glucosyl units for the substrate used in the present study, Fig. 2). By contrast, very little or no growth was observed on pullulan and amylopectin that contains longer branches (data not shown). Since *L. acidophilus* NCFM is only able to use the debranched maltose from β-limit dextrin, the energy yield per mass of this substrate is much lower compared to growth on maltose. Therefore, the observed low level of growth on β-limit dextrin is in agreement with the debranching activity of the cells and the lack of α-amylase activity that is required for the full-utilization of this susbtrate.

The poor growth on maltotriose and maltotetraose is, however, surprising as these substrates are predicted to be internalized through a maltodextrin specific ATP-binding cassette (ABC) system (LBA1864−LBA1867), which is conserved in acidophilus group lactobacilli (24). The corresponding transporter from the taxonomically related Gram-positive pathogen *Streptococcus pneumoniae* mediates the uptake of maltooligosaccharides up to eight units with a preference to maltotetraose (51). The expression of the ABC uptake system may be affected by an inserted transposase (LBA1868) that separates the catabolic genes from the transporter in *L. acidophilus* NCFM, but not in other lactobacilli (24). Nonetheless, the maltooligosaccharide uptake profile reveals that maltotriose and maltotetraose are taken up, albeit at a significantly slower rate than maltose (Fig. 3C) in *L. acidophilus* NCFM cultures. Growth experiments on two additional *L. acidophilus* strains confirmed that the strain possessing the transposase grew similarly poorly as *L.*

acidophilus NCFM, whereas the strain that lacks this insertion displayed better relative growth on maltotriose maltotetraose (Fig. S2).

Despite the weak growth, pullulanase activity was reliably measured during growth on maltotriose, maltotetraose and β-limit dextrin, but not on glucose (Fig. 3B). The pullulanase activity was detectable only in the cell fraction, providing evidence that the enzyme is cell attached. Thin layer chromatography analysis on samples from the pullulan assays with the cell fraction confirmed the pullulanase type debranching activity since the sole end product released was maltotriose. This precluded other enzymatic activities (*e.g.* neopullulanase or α-glucosidase) being responsible for the increase in reducing sugars from pullulan degradation (Fig. S3). The only predicted extracellular pullulanase in *L. acidophilus* NCFM is *La*Pul13_14 (locus tag LBA1710) (28). The inactivation of the gene encoding this enzyme abolished the cell attached pullulanase activity, providing compelling evidence that *La*Pul13_14 is the sole extracellular α-glucan debranching enzyme in *L. acidophilus* NCFM (Fig. 4).

The gene encoding *La*Pul13_14 resides on a separate locus than the maltodextrin utilization cluster (26). The repression of pullulanase activity in the presence of glucose is suggestive of regulation through global catabolite repression (52). Indeed, this enzyme was not identified in the exoproteome of *L. acidophilus* NCFM grown on glucose in a recent proteomic analysis of S-layer associated proteins (50). A similar observation was made in a proteome analysis of *L. acidophilus* NCFM grown on raffinose, where *La*Pul13_14 was repressed in the presence of glucose (53), but was clearly detectible in the presence of raffinose suggesting a level of constitutive expression of the enzyme in the absence of glucose.

La*Pul13_14 confers efficient targeting of small branched α-glucans.* Given the dominance of starch in human nutrition, the metabolism of this glucan by the HGM has been subject to extensive studies. *Ruminococcus bromii* has been identified as the primary degrader of resistant starch in the human gut (23), although *Bifidobacterium adolescentis* strains were also reported to possess growth capabilities on this substrate (15). Major commensals from the *Bacteroides genus* (54) and the

butyrate producing Firmicutes *Eubacterium rectale* (14) are other HGM with considerable starch growth and degradation capabilities. Common to these bacteria is that they possess highly modular extracellular cell-attached enzymes with one or more catalytic modules and multiple carbohydrate binding modules (CBMs), which mediate tight binding to starch substrates.

Only a few *Lactobacillus* strains have been demonstrated to utilize only soluble starch (18, 19, 55). This is in agreement with the rare occrence of genes encoding extracellular α-glucan enzymes in this genus (1.6% or 11 out of 696 GH13 genes). Notably, only four *Lactobacillus* species encode these extracellular enzymes: *L. acidophilus*, *Lactobacillus amylovorus*, *Lactobacillus plantarum*, and *Lactobacillus manihotivorans* (Table S1). *L. plantarum* and *L. amylophilus* GV6 possess amylopullulanases (pullulanase type II) that degrade both α-1,4- and α-1,6-branches in starch (56–58). Notably, these starch utilizing strains stem from other ecological niches than the human gut. By contrast, *La*Pul13_14 and its homologues that display an identical domain organization, represent the main extracellular amylolytic activity in human gut lactobacilli (Table S1). This unique modular organization and the presence of the SLAP domain in gut lactobacilli, raise a question on the importance of these enzymes in the gut niche.

The lack of activity of *La*Pul13_14 on granular starch and the very weak binding to this substrate (K_d >40 mg ml^{-1}, Fig. S1) are in line with the lack of growth of *L acidophilus* NCFM on starch. By contrast, the enzyme binds the starch mimic β-CD with moderate affinity (Table 2). This molecule occupies the conserved +2 substrate binding subsite in pullulanases, thus acting as a competitive inhibitor (41). Our β-CD inhibition kinetics data on pullulan reveal an inhibition constant K_i=36 µM, which is in the same range as the K_d obtained from surface plasmon resonance binding experiments (Table 2). More interestingly, the inhibition was not purely competitive but was of mixed nature (Fig. S4), indicative of the presence of additional α-glucan surface binding sites. The glucan-binding residues in the CBM41 of the pullulanases from *Streptococcus pneumoniae* (59) are conserved in *L. acidophilus* NCFM. This makes the CBM41 a plausible candidate for the additional α-glucan binding in *La*Pul13_14. A possible rationale for this additional binding in *La*Pul13_14 is

to increase substrate affinity by increasing the local substrate concentration in the proximity to the active site. Strikingly, the K_m of *La*Pul13_14 towards pullulan is the lowest reported for any debranching enzyme (Table S2), which attests adaptation of the susbtrate affinity to the competitive human gut niche. The clear preference for substrates with short branches of about two−three glucose units (Table 1) may provide a metabolic advantage for *L. acidophilus*, which is able to take-up and metabolize these substrates. Based on the kinetic parameters, the most likely substrates for *La*Pul13_14 are short branched α-glucans that are generated from the action of α-amylases on starch or glycogen. Given the poor digestibility of branched α-glucans by human enzymes and the abundance of lactobacilli in the small intestine (16), this enzyme may act on branched oligomeric substrates from human degradation of dietary starch or glycogen (Fig. 5). Such an advantage may explain the enrichment of this debranching activity in human intestinal isolates. Taken all together, the study suggests that debranching enzyme of gut lactobacilli are evolved for efficient breakdown of short branched α-glucans. The high substrate affinity may facilitate access to substrates that escape human or microbial metabolism of starch and glycogen. Further work is required to relate the *in vivo* functionality of these enzymes to gut adaptation of lactobacilli urther work is required to verify this.

A**CKNOWLEDGEMENTS**

Alexander Holm Viborg is acknowledged for providing us with bioinformatics tools for CAZyme analyses (ahv.dk). This work was supported by a grant from the Danish Strategic Research Council, Committee of Health and Nutrition, to the project “Gene Discovery and Molecular Interactions in Prebiotics/Probiotics Systems: Focus on Carbohydrate Prebiotics”. The Danish Council for Independent Research | Natural Sciences for the an instrument grant for the SPR.

REFERENCES

1. **Lozupone CA**, **Stombaugh JI**, **Gordon JI**, **Jansson JK**, **Knight R**. 2012. Diversity, stability and resilience of the human gut microbiota. Nature **489**:220–230.

2. **David LA**, **Maurice CF**, **Carmody RN**, **Gootenberg DB**, **Button JE**, **Wolfe BE**, **Ling A V**, **Devlin AS**, **Varma Y**, **Fischbach MA**, **Biddinger SB**, **Dutton RJ**, **Turnbaugh PJ**. 2014. Diet rapidly and reproducibly alters the human gut microbiome. Nature **505**:559–563.

3. **Martens EC**. 2016. Fibre for the future. Nature **529**:158–159.

4. **Sonnenburg JL**, **Bäckhed F**. 2016. Diet–microbiota interactions as moderators of human metabolism. Nature **535**:56–64.

5. **Hur KY**, **Lee M-S**. 2015. Gut microbiota and metabolic disorders. Diabetes Metab J **39**:198–203.

6. **Flint HJ**, **Scott KP**, **Duncan SH**, **Louis P**, **Forano E**. 2012. Microbial degradation of complex carbohydrates in the gut. Gut Microbes **3**:289–306.

7. **Koropatkin NM**, **Cameron EA**, **Martens EC**. 2012. How glycan metabolism shapes the human gut microbiota. Nat Rev Microbiol **10**:323–335.

8. **Tester RF**, **Karkalas J**, **Qi X**. 2004. Starch–composition, fine structure and architecture. J Cereal Sci **39**:151–165.

9. **Møller MS**, **Goh YJ**, **Viborg AH**, **Andersen JM**, **Klaenhammer TR**, **Svensson B**, **Abou Hachem M**. 2014. Recent insight in α-glucan metabolism in probiotic bacteria. Biologia (Bratisl) **69**:713–721.

10. **Blazek J**, **Gilbert EP**. 2010. Effect of enzymatic hydrolysis on native starch granule structure. Biomacromolecules **11**:3275–3289.

11. **Zhang G**, **Hamaker BR**. 2009. Slowly digestible starch: concept, mechanism, and proposed extended glycemic index. Crit Rev Food Sci Nutr **49**:852–867.

12. **Fuentes-Zaragoza E**, **Sánchez-Zapata E**, **Sendra E**, **Sayas E**, **Navarro C**, **Fernández-López J**, **Pérez-Alvarez JA**. 2011. Resistant starch as prebiotic: A review. Starch - Stärke **63**:406–415.

13. **Cockburn DW**, **Koropatkin NM**. 2016. Polysaccharide degradation by the intestinal microbiota and its influence on human health and disease. J Mol Biol **428**:3230–3252.

14. **Cockburn DW**, **Orlovsky NI**, **Foley MH**, **Kwiatkowski KJ**, **Bahr CM**, **Maynard M**, **Demeler B**, **Koropatkin NM**. 2015. Molecular details of a starch utilization pathway in the human gut symbiont *Eubacterium rectale*. Mol Microbiol **95**:209–230.

15. **Leitch ECM**, **Walker AW**, **Duncan SH**, **Holtrop G**, **Flint HJ**. 2007. Selective colonization of insoluble substrates by human faecal bacteria. Environ Microbiol **9**:667–679.

16. **Donaldson GP**, **Lee SM**, **Mazmanian SK**. 2016. Gut biogeography of the bacterial microbiota. Nat Rev Microbiol **14**:20–32.

17. **Bull M**, **Plummer S**, **Marchesi J**, **Mahenthiralingam E**. 2013. The life history of *Lactobacillus acidophilus* as a probiotic: a tale of revisionary taxonomy, misidentification and commercial success. FEMS Microbiol Lett **349**:77–87.

18. **Petrova P**, **Petrov K**, **Stoyancheva G**. 2013. Starch-modifying enzymes of lactic acid bacteria – structures, properties, and applications. Starch - Stärke **65**:34–47.

19. **Velikova P**, **Stoyanov A**, **Blagoeva G**, **Popova L**, **Petrov K**, **Gotcheva V**, **Angelov A**, **Petrova P**. 2016. Starch utilization routes in lactic acid bacteria: new insight by gene expression assay. Starch - Stärke **68**:1–8.

20. **Wang X**, **Brown IL**, **Khaled D**, **Mahoney MC**, **Evans AJ**, **Conway PL**. 2002. Manipulation of colonic bacteria and volatile fatty acid production by dietary high amylose maize (amylomaize) starch granules. J Appl Microbiol **93**:390–397.

21. **Le Blay GM**, **Michel CD**, **Blottière HM**, **Cherbut CJ**. 2003. Raw potato starch and short-chain fructo-oligosaccharides affect the composition and metabolic activity of rat intestinal

506 microbiota differently depending on the caecocolonic segment involved. J Appl Microbiol
507 **94**:312–320.

508 22. **Ordiz MI**, **May TD**, **Mihindukulasuriya K**, **Martin J**, **Crowley J**, **Tarr PI**, **Ryan K**,
509 **Mortimer E**, **Gopalsamy G**, **Maleta K**, **Mitreva M**, **Young G**, **Manary MJ**. 2015. The
510 effect of dietary resistant starch type 2 on the microbiota and markers of gut inflammation in
511 rural Malawi children. Microbiome **3**:1–9.

512 23. **Ze X**, **Duncan SH**, **Louis P**, **Flint HJ**. 2012. *Ruminococcus bromii* is a keystone species for
513 the degradation of resistant starch in the human colon. ISME J **6**:1535–1543.

514 24. **Møller MS**, **Fredslund F**, **Majumder A**, **Nakai H**, **Poulsen J-CN**, **Lo Leggio L**, **Svensson**
515 **B**, **Abou Hachem M**. 2012. Enzymology and structure of the GH13_31 glucan 1,6-α-
516 glucosidase that confers isomaltooligosaccharide utilization in the probiotic *Lactobacillus*
517 *acidophilus* NCFM. J Bacteriol **194**:4249–4259.

518 25. **Andersen JM**, **Barrangou R**, **Hachem MA**, **Lahtinen SJ**, **Goh Y-J**, **Svensson B**,
519 **Klaenhammer TR**. 2012. Transcriptional analysis of prebiotic uptake and catabolism by
520 *Lactobacillus acidophilus* NCFM. PLoS One **7**:e44409.

521 26. **Nakai H**, **Baumann MJ**, **Petersen BO**, **Westphal Y**, **Schols H**, **Dilokpimol A**, **Abou**
522 **Hachem M**, **Lahtinen SJ**, **Duus JØ**, **Svensson B**. 2009. The maltodextrin transport system
523 and metabolism in *Lactobacillus acidophilus* NCFM and production of novel α-glucosides
524 through reverse phosphorolysis by maltose phosphorylase. FEBS J **276**:7353–7365.

525 27. **Altermann E**, **Russell WM**, **Azcarate-Peril MA**, **Barrangou R**, **Buck BL**, **McAuliffe O**,
526 **Souther N**, **Dobson A**, **Duong T**, **Callanan M**, **Lick S**, **Hamrick A**, **Cano R**,
527 **Klaenhammer TR**. 2005. Complete genome sequence of the probiotic lactic acid bacterium
528 *Lactobacillus acidophilus* NCFM. Proc Natl Acad Sci U S A **102**:3906–3912.

529 28. **Lombard V**, **Golaconda Ramulu H**, **Drula E**, **Coutinho PM**, **Henrissat B**. 2014. The
530 carbohydrate-active enzymes database (CAZy) in 2013. Nucleic Acids Res **42**:490–495.

29. **Marchler-Bauer A**, **Derbyshire MK**, **Gonzales NR**, **Lu S**, **Chitsaz F**, **Geer LY**, **Geer RC**, **He J**, **Gwadz M**, **Hurwitz DI**, **Lanczycki CJ**, **Lu F**, **Marchler GH**, **Song JS**, **Thanki N**, **Wang Z**, **Yamashita R a.**, **Zhang D**, **Zheng C**, **Bryant SH**. 2015. CDD: NCBI's conserved domain database. Nucleic Acids Res **43**:D222–D226.

30. **Bertoldo C**, **Antranikian A**. 2002. Starch-hydrolyzing enzymes from thermophilic archaea and bacteria. Curr Opin Chem Biol **6**:151–160.

31. **Domań-Pytka M**, **Bardowski J**. 2004. Pullulan degrading enzymes of bacterial origin. Crit Rev Microbiol **30**:107–121.

32. **Møller MS**, **Henriksen A**, **Svensson B**. 2016. Structure and function of α-glucan debranching enzymes. Cell Mol Life Sci **73**:2619–2641.

33. **Finn RD**, **Coggill P**, **Eberhardt RY**, **Eddy SR**, **Mistry J**, **Mitchell AL**, **Potter SC**, **Punta M**, **Qureshi M**, **Sangrador-Vegas A**, **Salazar GA**, **Tate J**, **Bateman A**. 2016. The Pfam protein families database: towards a more sustainable future. Nucleic Acids Res **44**:D279–D285.

34. **Petersen TN**, **Brunak S**, **von Heijne G**, **Nielsen H**. 2011. SignalP 4.0: discriminating signal peptides from transmembrane regions. Nat Methods **8**:785–786.

35. **Kimmel SA**, **Roberts RF**. 1998. Development of a growth medium suitable for exopolysaccharide production by *Lactobacillus delbrueckii* ssp. *bulgaricus* RR. Int J Food Microbiol **40**:87–92.

36. **Goh YJ**, **Andrea Azcárate-Peril M**, **O'Flaherty S**, **Durmaz E**, **Valence F**, **Jardin J**, **Lortal S**, **Klaenhammer TR**. 2009. Development and application of a *upp*-based counterselective gene replacement system for the study of the S-layer protein SlpX of *Lactobacillus acidophilus* NCFM. Appl Environ Microbiol **75**:3093–3105.

37. **Horton RM**, **Hunt HD**, **Ho SN**, **Pullen JK**, **Pease LR**. 1989. Engineering hybrid genes without the use of restriction enzymes: gene splicing by overlap extension. Gene **77**:61–68.

38. **Goh YJ**, **Klaenhammer TR**. 2010. Functional roles of aggregation-promoting-like factor in stress tolerance and adherence of *Lactobacillus acidophilus* NCFM. Appl Environ Microbiol **76**:5005–5012.

39. **Fredslund F**, **Abou Hachem M**, **Jonsgaard Larsen R**, **Gerd Sørensen P**, **Coutinho PM**, **Lo Leggio L**, **Svensson B**. 2011. Crystal structure of α-galactosidase from *Lactobacillus acidophilus* NCFM: Insight into tetramer formation and substrate binding. J Mol Biol **412**:466–480.

40. **Barkholt V**, **Jensen AL**. 1989. Amino acid analysis: Determination of cysteine plus half-cystine in proteins after hydrochloric acid hydrolysis with a disulfide compound as additive. Anal Biochem **177**:318–322.

41. **Vester-Christensen MB**, **Abou Hachem M**, **Naested H**, **Svensson B**. 2010. Secretory expression of functional barley limit dextrinase by *Pichia pastoris* using high cell-density fermentation. Protein Expr Purif **69**:112–119.

42. **Sanders ME**, **Klaenhammer TR**. 2001. Invited review: the scientific basis of *Lactobacillus acidophilus* NCFM functionality as a probiotic. J Dairy Sci **84**:319–31.

43. **O'Flaherty S**, **Klaenhammer TR**. 2010. The role and potential of probiotic bacteria in the gut, and the communication between gut microflora and gut/host. Int Dairy J **20**:262–268.

44. **Leyer GJ**, **Li S**, **Mubasher ME**, **Reifer C**, **Ouwehand AC**. 2009. Probiotic effects on cold and influenza-like symptom incidence and duration in children. Pediatrics **124**:e172–e179.

45. **Ringel-Kulka T**, **Palsson OS**, **Maier D**, **Carroll I**, **Galanko JA**, **Leyer G**, **Ringel Y**. 2011. Probiotic bacteria *Lactobacillus acidophilus* NCFM and *Bifidobacterium lactis* Bi-07 versus placebo for the symptoms of bloating in patients with functional bowel disorders: a double-blind study. J Clin Gastroenterol **45**:518–525.

46. **Andersen JM**, **Barrangou R**, **Abou Hachem M**, **Lahtinen S**, **Goh YJ**, **Svensson B**, **Klaenhammer TR**. 2011. Transcriptional and functional analysis of galactooligosaccharide

uptake by *lacS* in Lactobacillus acidophilus. Proc Natl Acad Sci **108**:17785–17790.

47. **Barrangou R**, **Azcarate-Peril MA**, **Duong T**, **Conners SB**, **Kelly RM**, **Klaenhammer TR**. 2006. Global analysis of carbohydrate utilization by *Lactobacillus acidophilus* using cDNA microarrays. Proc Natl Acad Sci U S A **103**:3816–3821.

48. **Johnson BR**, **Klaenhammer TR**. 2016. AcmB is an S-layer-associated β-N-acetylglucosaminidase and functional autolysin in *Lactobacillus acidophilus* NCFM. Appl Environ Microbiol **82**:5687–5697.

49. **Hynönen U**, **Palva A**. 2013. *Lactobacillus* surface layer proteins: structure, function and applications. Appl Microbiol Biotechnol **97**:5225–5243.

50. **Johnson BR**, **Hymes J**, **Sanozky-Dawes R**, **DeCrescenzo Henriksen E**, **Barrangou R**, **Klaenhammer TR**. 2016. Conserved S-layer-associated proteins revealed by exoproteomic survey of S-layer-forming lactobacilli. Appl Environ Microbiol **82**:134–145.

51. **Abbott DW**, **Higgins MA**, **Hyrnuik S**, **Pluvinage B**, **Lammerts van Bueren A**, **Boraston AB**. 2010. The molecular basis of glycogen breakdown and transport in *Streptococcus pneumoniae*. Mol Microbiol **77**:183–199.

52. **Mahr K**, **Hillen W**, **Titgemeyer F**. 2000. Carbon catabolite repression in *Lactobacillus pentosus*: analysis of the *ccpA* region. Appl Environ Microbiol **66**:277–283.

53. **Celebioglu HU**, **Ejby M**, **Majumder A**, **Køble C**, **Goh YJ**, **Schmidt B**, **O'Flaherty S**, **Abou Hachem M**, **Lahtinen SJ**, **Jacobsen S**, **Klaenhammer TR**, **Brix S**, **Mølhave K**, **Svensson B**. 2016. Differential proteome and cellular adhesion analyses of the probiotic bacterium *Lactobacillus acidophilus* NCFM grown on raffinose – an emerging prebiotic. Proteomics **16**:1361–1375.

54. **Cameron EA**, **Maynard MA**, **Smith CJ**, **Smith TJ**, **Koropatkin NM**, **Martens EC**. 2012. Multidomain carbohydrate-binding proteins involved in *Bacteroides thetaiotaomicron* starch metabolism. J Biol Chem **287**:34614–34625.

606 55. **Lee HS**, **Gilliland SE**, **Carter S**. 2001. Amylolytic cultures of *Lactobacillus acidophilus*:
607 potential probiotics to improve dietary starch utilization. Food Microbiol Saf **66**:338–344.

608 56. **Kim J-H**, **Sunako M**, **Ono H**, **Murooka Y**, **Fukusaki E**, **Yamashita M**. 2008.
609 Characterization of gene encoding amylopullulanase from plant-originated lactic acid
610 bacterium, *Lactobacillus plantarum* L137. J Biosci Bioeng **106**:449–459.

611 57. **Kim J-H**, **Sunako M**, **Ono H**, **Murooka Y**, **Fukusaki E**, **Yamashita M**. 2009.
612 Characterization of the C-terminal truncated form of amylopullulanase from *Lactobacillus*
613 *plantarum* L137. J Biosci Bioeng **107**:124–129.

614 58. **Vishnu C**, **Naveena BJ**, **Altaf M**, **Venkateshwar M**, **Reddy G**. 2006. Amylopullulanase—
615 A novel enzyme of *L. amylophilus* GV6 in direct fermentation of starch to L(+) lactic acid.
616 Enzyme Microb Technol **38**:545–550.

617 59. **Lammerts van Bueren A**, **Ficko-Blean E**, **Pluvinage B**, **Hehemann J-H**, **Higgins MA**,
618 **Deng L**, **Ogunniyi AD**, **Stroeher UH**, **El Warry N**, **Burke RD**, **Czjzek M**, **Paton JC**,
619 **Vocadlo DJ**, **Boraston AB**. 2011. The conformation and function of a multimodular
620 glycogen-degrading pneumococcal virulence factor. Structure **19**:640–651.

621

622 **TABLES**

TABLE 1. Hydrolysis kinetic parameters of *La*Pul13_14 towards oligomeric and polymeric α-1,6-branched glucans at 37°C and pH 5.0.

Substrate	K_m	k_{cat}	$k_{cat}\ K_m^{-1}$	**Normalized** $k_{cat}\ K_m^{-1}$
	$mg\ ml^{-1}$	s^{-1}	$ml\ s^{-1}\ mg^{-1}$	
Pullulan	0.05±0.004	518±10.5	10368	100
Amylopectin	0.37±0.041	25±0.7	67	0.6
β-limit dextrin	0.20±0.090	189±15.8	945	9
6^2-α-D-maltosyl maltotriose	0.33±0.040[a]	378±18.0[b]	1145[c]	

[a] *mM*; [b] s^{-1}; [c] $mM^{-1}s^{-1}$

623

TABLE 1. Binding of cyclodextrins to *La*Pul13_14 determined by surface plasmon resonance.

Cyclic Ligand	pH	Temperature (°C)	K_D (μM)
α-CD	5.0	25	89.0
γ-CD	5.0	25	11.2
β-CD	5.0	25	10.8
β-CD	5.0	15	7.2
β-CD	5.0	37	29.9
β-CD	7.0	25	21.8

624

FIGURES

FIG 1 Domain organization of *La*Pul13_14. The abbreviations are: SP, signal peptide; CBM41, starch binding module of CBM41 in the CAZy database; N-dom, N-terminal domain of unknown function; CBM48, starch binding module of CBM48; GH13_14, catalytic module assigned into glycoside hydrolase family 13 subfamily 14; C-terminal domain conserved in pullulanases of GH13; SLAP, surface layer association protein domain.

FIG 2 Schematic overview of α-glucans included in the present study. α-1,4-linked glucose units are shown as linear hexagons and α-1,6-linkages are depicted as horizontal short segments between the glucosyl unit hexagons with the reducing end depicted as a white hexagon. The small branched α-limit dextrin is resembling the one used in this study. β-Limit dextrin, produced from β-amylase hydrolysis of amylopectin is used to provide experimental evidence for the preference of the *La*Pul13_14 to short branches compared to amylopectin.

FIG 3 (A) Growth of *L. acidophilus* NCFM on different α-glucans and (B) the relative cell-associated pullulan hydrolyzing activity of *L. acidophilus* NCFM cells harvested after 10 h of growth on the α-glucans shown in (A). (C) Growth of *L. acidophilus* NCFM on a total of 0.5% (w/v) mixture of maltose, maltotriose, and maltotetraose (1:1:1 based on weight), and its utilization of the substrates was analysed by HPAEC-PAD. Only the debranched mainly maltose and maltotriose are used from β-Limit dextrin during growth on this substrate, which explains the much lower degree of growth per mass substrate as compared to maltose.

FIG 4 (A) Comparison of the growth of wildtype *L. acidophilus* NCFM and the *La*Pul13_14 gene deletion strain (ΔLBA1710) on glucose or maltose, and (B) the cell-associated pullulan hydrolyzing activity of cells harvested after 10 h of growth.

FIG 5 Schematic overview of the extracellular α-glucan metabolism of *L. acidophilus* NCFM. The cell-attached pullulanase activity of *La*Pul13_14 mediates the debranching of preferentially smaller branched oligomers that possibly are products from human or bacterial degradation of amylopectin, which is signified by a dashed line. The produced maltose and short maltooligosaccharides are

651 taken up by one or more specific transporters and degraded intracellularly by the enzymes encoded
652 by the maltooligosaccharide utilization locus to produce β-glucose-1-phosphate and glucose, which
653 enter glycolysis (26).


SP
CBM41
N-dom
CBM48
Catalytic domain
C-dom
SLAP
1185 aa

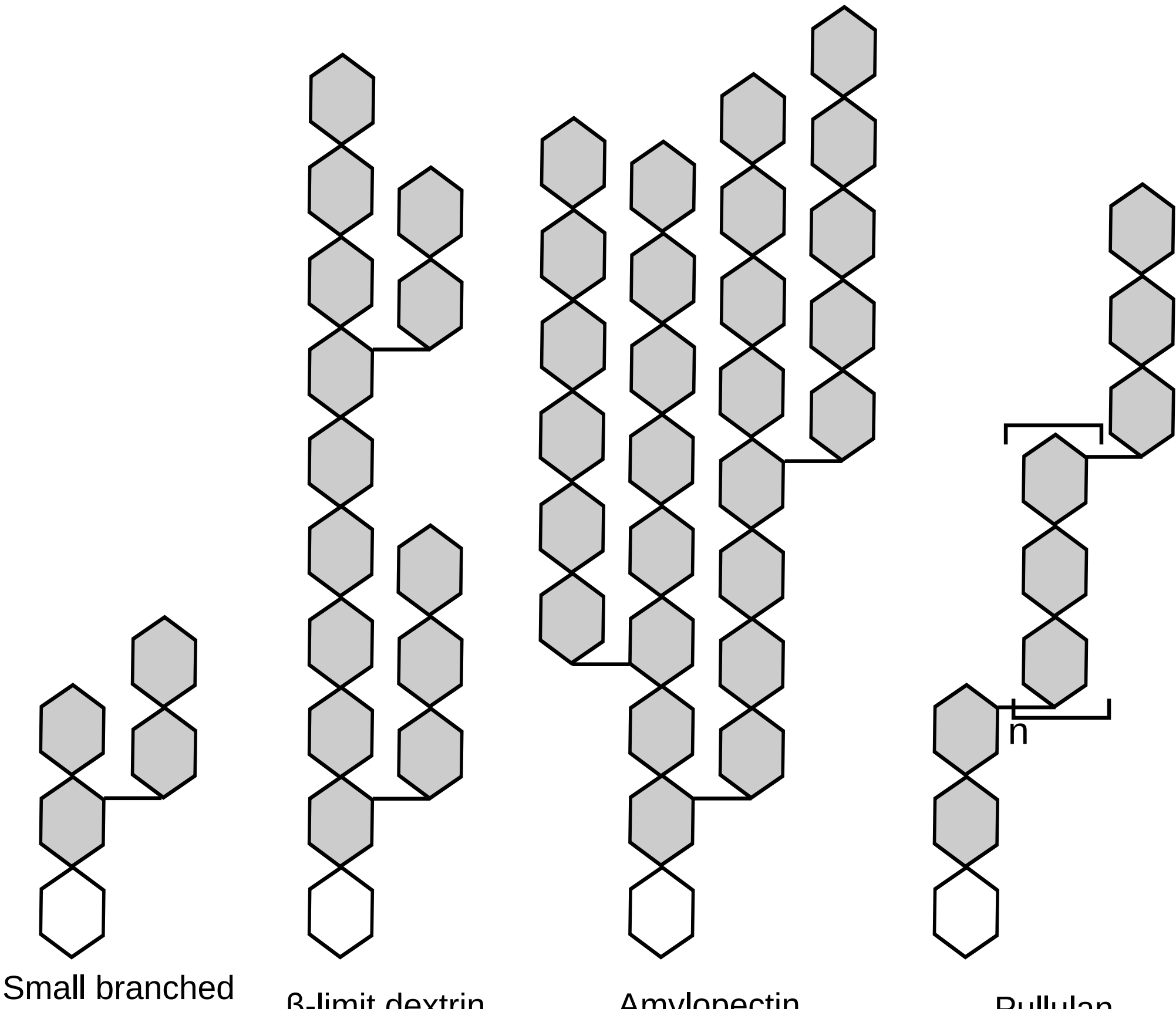

Small branched α-limit dextrin

β-limit dextrin

Amylopectin

Pullulan

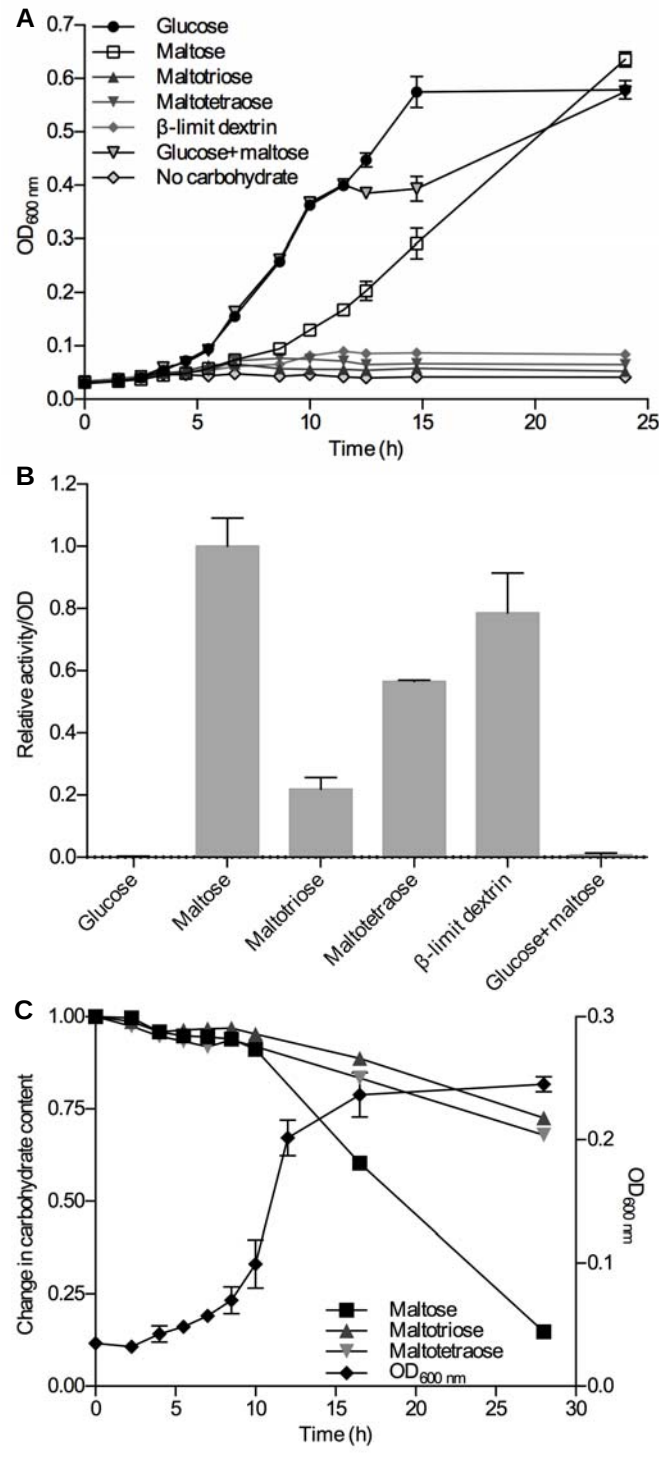
A
Glucose
Maltose
Maltotriose
Maltotetraose
β-limit dextrin
Glucose+maltose
No carbohydrate
OD600 nm
Time (h)
B
Relative activity/OD
Glucose
Maltose
Maltotriose
Maltotetraose
β-limit dextrin
Glucose+maltose
C
Change in carbohydrate content
OD600 nm
Maltose
Maltotriose
Maltotetraose
OD600 nm
Time (h)

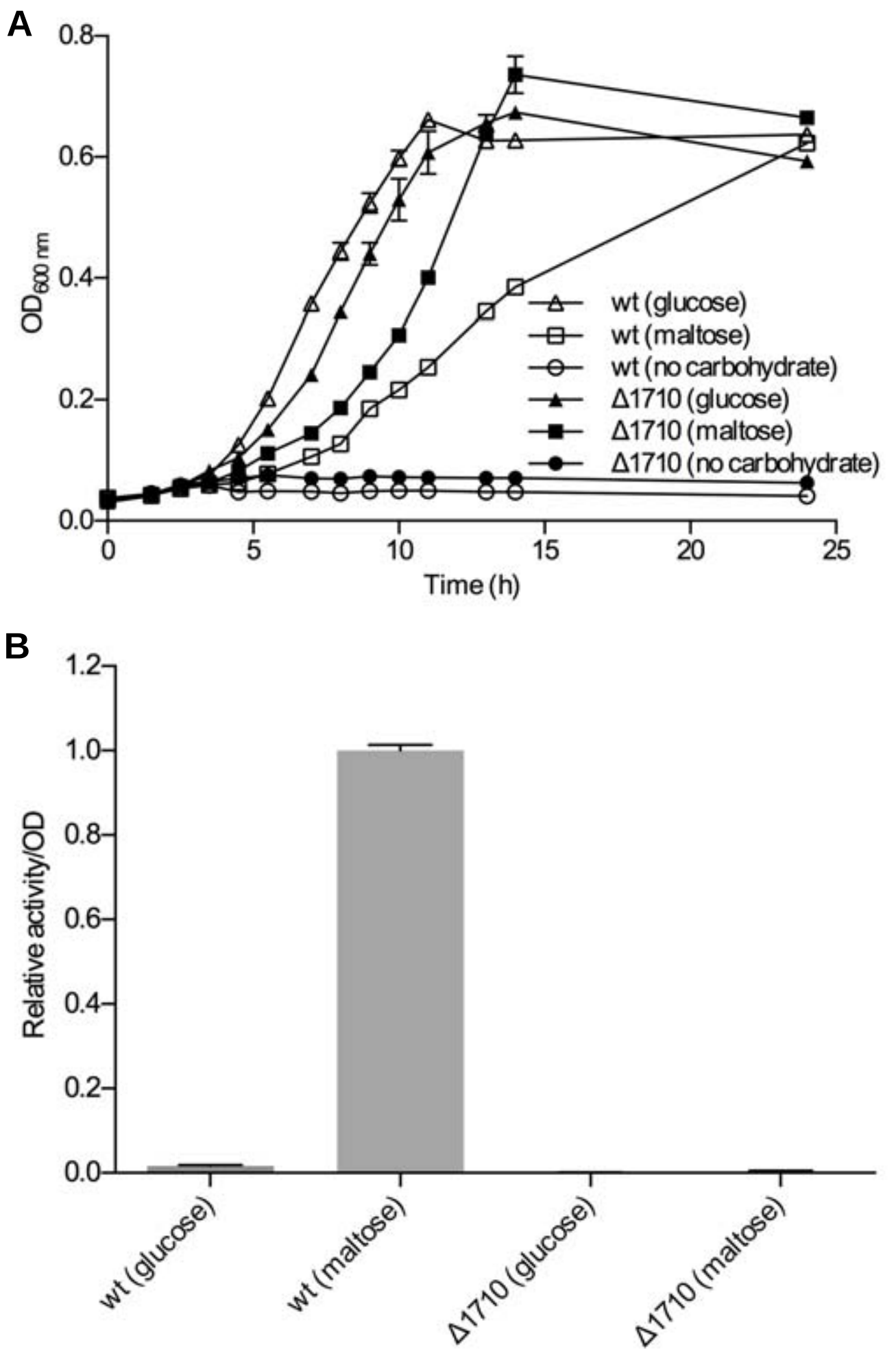
A
0.8
0.6
0.4
0.2
0.0
OD600 nm
0
5
10
15
20
25
Time (h)
wt (glucose)
wt (maltose)
wt (no carbohydrate)
Δ1710 (glucose)
Δ1710 (maltose)
Δ1710 (no carbohydrate)
B
1.2
1.0
0.8
0.6
0.4
0.2
0.0
Relative activity/OD
wt (glucose)
wt (maltose)
Δ1710 (glucose)
Δ1710 (maltose)

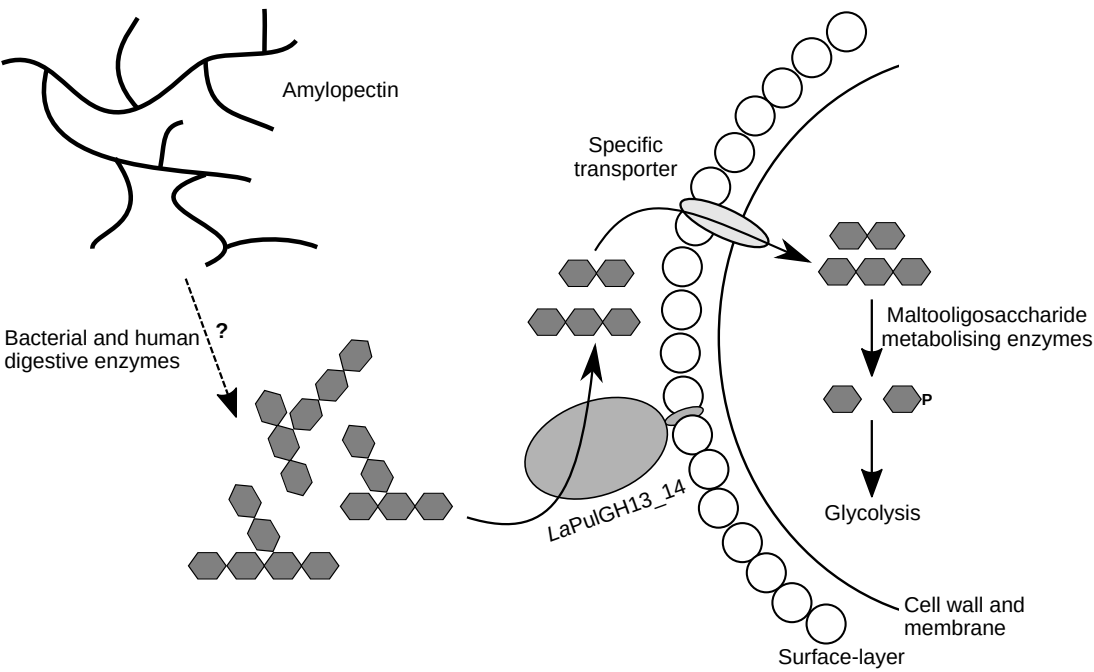
Amylopectin
Specific
transporter
Bacterial and human
digestive enzymes
?
Maltooligosaccharide
metabolising enzymes
P
Glycolysis
LaPulGH13_14
Cell wall and
membrane
Surface-layer

SUPPLEMENTAL MATERIAL

An extracellular cell-attached pullulanase confers branched α-glucan utilization in the human gut probiotic *Lactobacillus acidophilus* NCFM

Marie S. Møller,[a] Yong Jun Goh,[b] Kasper Bøwig Rasmussen,[a]* Wojciech Cypryk,[a]* Hasan Ufuk Celebioglu,[a] Todd R. Klaenhammer,[b] Birte Svensson,[a] Maher Abou Hachem[a]#

Department of Biotechnology and Biomedicine, Technical University of Denmark, Kgs. Lyngby, Denmark[a]; Department of Food, Bioprocessing and Nutrition Sciences, North Carolina State University, Raleigh, North Carolina[b]

#Address correspondence to Maher Abou Hachem, maha@bio.dtu.dk and Yong Jun Goh yjgoh@ncsu.edu.
*Present address: Kasper Bøwig Rasmussen, Novo Nordisk A/S, Gentofte, Denmark; Wojciech Cypryk, Department of Bioorganic Chemistry, Polish Academy of Sciences, Lodz, Poland.

Table S1. Predicted extracellular enzymes (SignalP (1)) of GH13 from available *Lactobacillus* genomes.

Genbank accession	**Organism**	**GH13 subfamily[a]**	**SLAP domain[b]**	**Isolate origin**
AAV43522	*L. acidophilus* NCFM	14	+	**Human gut**
AJP47013	*L. acidophilus* FSI4	14	+	Yogurt
AGK94861	*L. acidophilus* La-14	14	+	**Human gut**
ADZ06675	*L. amylovorus* 30SC	14	+	**Porcine gut**
ADQ58495	*L. amylovorus* GRL1112	14	+	**Porcine gut**
AEA31469	*L. amylovorus* GRL1118	14	+	**Porcine ileum**
AAC45781	*L. amylovorus* CIP 102989	28	-	Cattle (waste-corn fermentation)
AAD45245	*L. manihotivorans* LMG 18010T	28	-	Cassava
AAC45780	*L. plantarum* A6	28	-	Cassava
BAF93906	*L. plantarum* L137	14	-	Fermented food
AHX97726	*L. plantarum* S21	28	-	Fermented rice noodles

[a]Subfamily classification in the CAZy data base (www.CAZy.org).
[b]The occurrence of a surface layer association protein domain in the enzyme is denoted by "+"

Table S2. Comparison of kinetic parameters of pullulanases. Purple, GH13_13, i.e. enzymes mainly acting on β-limit dextrins; Blue, GH13_14, i.e. enzymes with activity on β-limit dextrins as well as the polymeric α-glucans amylopectin and glycogen; Orange, Unclassified/no protein sequence in CAZy. The enzyme from *L. acidophilus* NCFM displays the highest catalytic efficiency for any debranching enzyme owing to an unprecedented low K_m.

Organism	pH, temperature	K_m *mg ml^{-1}*	k_{cat} *s^{-1}*	k_{cat}/K_m *ml s^{-1} mg^{-1}*	Reference
PULLULAN					
Barley (*Hordeum vulgare*)	5.5, 37°C	0.081±0.003	61±13	753	(2)
Klebsiella pneumoniae,	5.0, 40°C	0.017	103.3	6076	(3)
Klebsiella pneumoniae	5.4, 37°C	0.617	116	188	(4)
Rice (*Oryza sativa* L. *japonica*)	6.0, 37°C	0.625	23.1	37.0	(5)
Spinach *(Spinacia oleracea)*	6.0, 37°C	0.78/0.70			(6, 7)
Anaerobranca gottschalkii	8, 60°C	0.75			(8)
Bacillus acidopullulyticus	5.0, 70°C	4.0			(9)
Bacillus deramificans	4.5, 60°C	0.70±0.02	1900.4±103.5	2712.9±121.6	(10)
Bacillus subtilis strain 168	5.4, 37°C	1.284	97	75.5	(4)
Exiguobacterium sp. SH3	7.0, 37°C	0.069			(11)
Fervidobacterium pennavorans	6.0, 80°C	0.4			(12)
***Lactobacillus acidophilus* NCFM**	**5.0, 37°C**	**0.05±0.004**	**518.4±10.5**	**10368**	**This study**
Paenibacillus barengoltzi	5.5, 50°C	2.94			(13)
Paenibacillus polymyxa Nws-pp2	6.0, 35°C	15.25			(14)
Bacillus cereus Nws-bc5	7.0, 40°C	0.45			(15)
Bacillus megaterium WW1210	6.5, 55°C	3.3±0.25			(16)
Bacillus naganoensis	4.5, 60°C	1.22±0.11	0.72±0.01	0.59	(17)
Bacillus sp. AN-7	6, 80°C	1.3			(18)
Bacillus sp. S-1	9.0, 50°C	7.92			(19)
Thermoanaerobacter thermohydrosulfuricus (Clostridium thermohydrosulfuricum)	6.0, 60°C	0.675	271	410	(20)
Exiguobacterium acetylium a1/YH5	6.0, 50°C	0.12±0.02			(21)
Lactococcus lactis IBB 500	4.5, 60°C	0.34±0.02			(22)
Oat (*Avena sativa*)	5.0, 30°C	0.17			(23)
Sorghum bicolor	5.0, 30°C	0.2			(24)
Sugar beet (*Beta vulgaris* var. *altissima*)	5.6, 37°C	0.31			(25)
Thermus caldophilus GK-24	7.0, 73°C	0.42			(26)
POTATO AMYLOPECTIN					
Barley (*Hordeum vulgare*)	5.5, 37°C	6.9±1.0	15.6±1.2	2.3	(27)
Klebsiella pneumoniae	5.5, 40°C	10.1	14.1		(3)
Rice (*Oryza sativa* L. *japonica*)	6.0, 37°C	1.538			(5)
Spinach (*Spinacia oleracea*)	6.0, 37°C	7			(6, 7)
***Lactobacillus acidophilus* NCFM**	**5.0, 37°C**	**0.37±0.041**	**24.9±0.7**	**67**	**This study**
Bacillus megaterium WW1210	6.5, 55°C	3.6±0.18			(16)
Bacillus sp. S-1	9.0, 50°C	1.63			(19)
Broad bean (*Vicia faba* L.)	30°C	1.2			(28)
Oat (*Avena sativa*)	5.0, 30°C	1.4			(23)
Sugar beet (*Beta vulgaris* var. *altissima*)	5.6, 37°C	4.55			(25)
AMYLOPECTIN β-LIMIT DEXTRIN					
Broad bean (*Vicia faba* L.)	30°C	1			(28)
Sorghum bicolor	5.0, 37°C	2.5			(24)
***Lactobacillus acidophilus* NCFM**	**5.0, 37°C**	**0.20±0.090**	**189±15.8**	**945**	**This study**

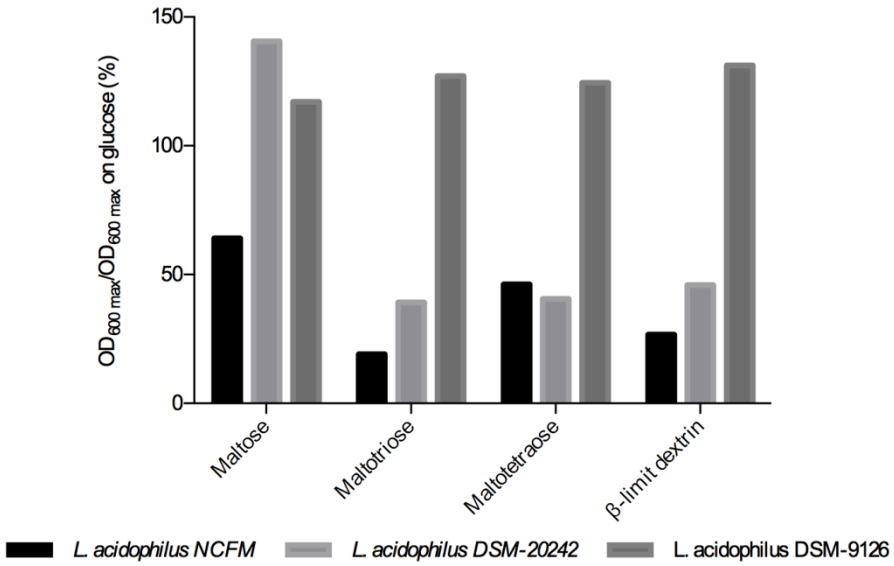

Fig. S1. Maximal growth of three *L. acidophilus* strains on maltooligosaccharides and β-limit dextrin relative to the maximal growth on glucose. *L. acidophilus* NCFM and *L. acidophilus* DSM-20242 have a comparable maltooligosaccharides utilisation gene cluster, *i.e.* they have a transposase included in the cluster. The *L. acidophilus* DSM-9126 does not have a transposase in its maltooligosaccharides utilisation gene cluster, and is likely to have an intact expression of the ATP-binding cassette transporter.

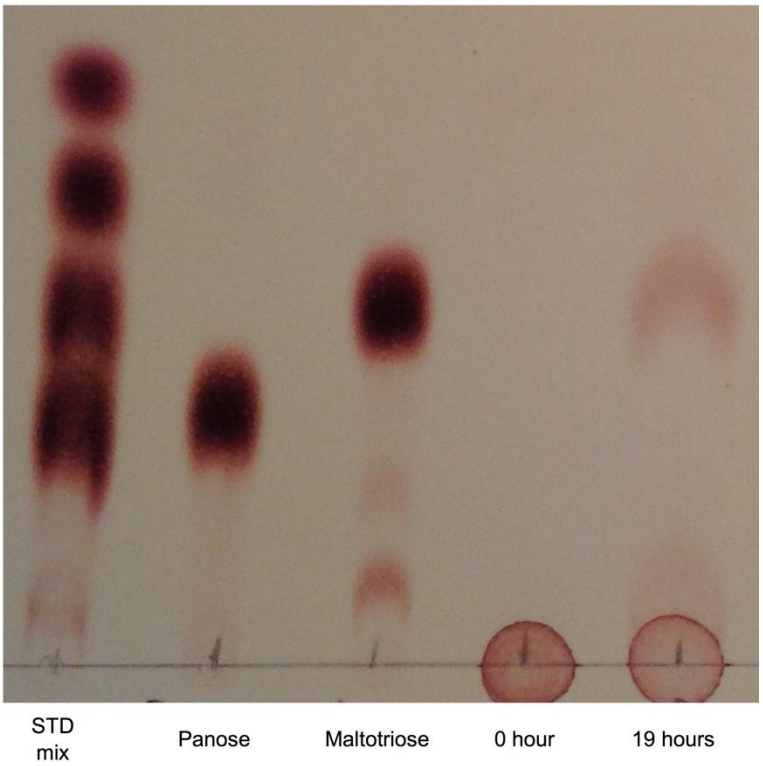

Fig. S2. Thin layer chromatography analysis of the degradation product from whole cell assay with pullulan. The standard mix (STD mix) consists of 20 mM of (mentioned from the top); glucose, maltose, maltotriose, panose. Furthermore, 20 mM panose and 20 mM maltotriose were spotted separately. The plate clearly shows the exclusive release of maltotriose after 19 h (first lane on the right side of the plate), confirming the pullulanase activity.

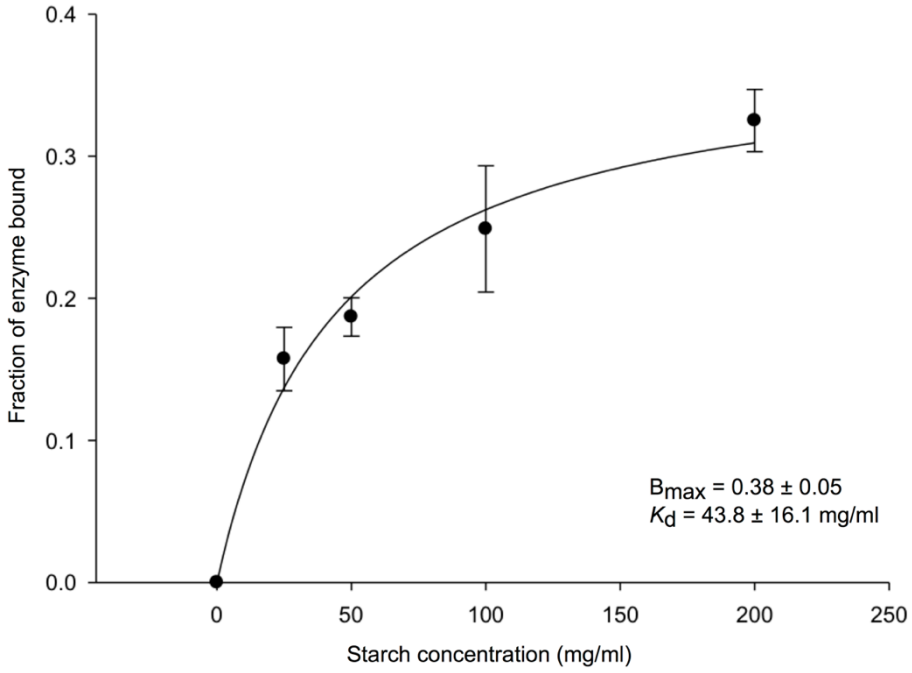

Fig. S3. Binding of *La*Pul13_14 to starch granules. The data is from four replicate experiments. The solid line is the fit of a one binding site model to the data, with the B_{max} and the K_d as the maximum binding capacity and dissociation constant, respectively.

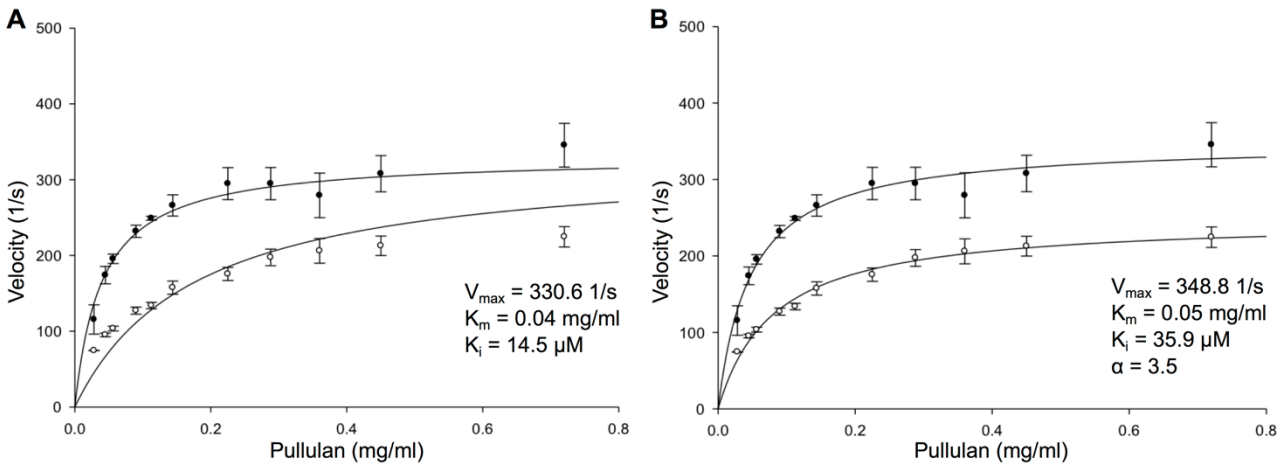

Fig. S4. Inhibition kinetics of *La*Pul13_14 on pullulan by β-cyclodextrin (50 µM). Two different inhibition models are shown. The solid and hollow circles represent the initial rates in the absence and the presence of β-cyclodextrin, respectively. The solid lines represent the fit to: (A) a competitive inhibition model and (B) mixed inhibition model. The competitive inhibition model results is systematic poor fits to the data, whereas the data is well modelled by a mixed inhibition model, which is the best model also as compared to a non-competitive inhibition model (not shown).

REFERENCES:

1. **Petersen TN**, **Brunak S**, **von Heijne G**, **Nielsen H**. 2011. SignalP 4.0: discriminating signal peptides from transmembrane regions. Nat Methods **8**:785–786.

2. **Vester-Christensen MB**, **Abou Hachem M**, **Naested H**, **Svensson B**. 2010. Secretory expression of functional barley limit dextrinase by *Pichia pastoris* using high cell-density fermentation. Protein Expr Purif **69**:112–119.

3. **Yokobayashi K**, **Akai H**, **Sugimoto T**, **Hirao M**, **Sugimoto K**, **Harada T**. 1973. Comparison of the kinetic parameters of *Pseudomonas* isoamylase and *Aerobacter* pullulanase. Biochim Biophys Acta **293**:197–202.

4. **Malle D**, **Itoh T**, **Hashimoto W**, **Murata K**, **Utsumi S**, **Mikami B**. 2006. Overexpression, purification and preliminary X-ray analysis of pullulanase from *Bacillus subtilis* strain 168. Acta Crystallogr Sect F Struct Biol Cryst Commun **62**:381–384.

5. **Yamasaki Y**, **Nakashima S**, **Konno H**. 2008. Pullulanase from rice endosperm. Acta Biochim Pol **55**:507–510.

6. **Ludwig I**, **Ziegler P**, **Beck E**. 1984. Purification and properties of spinach leaf debranching enzyme. Plant Physiol **74**:856–861.

7. **Renz A**, **Schikora S**, **Schmid R**, **Kossmann J**, **Beck E**. 1998. cDNA sequence and heterolohous expression of monomeric spinnach pullulanase: multiple isomeric forms arise from the same polypeptide. Biochem J **331**:937–945.

8. **Bertoldo C**, **Armbrecht M**, **Becker F**, **Scha T**, **Antranikian G**, **Liebl W**. 2004. Cloning, sequencing, and characterization of a heat- and alkali-stable type I pullulanase from *Anaerobranca gottschalkii*. Appl Environ Microbiol **70**:3407–3416.

9. **Singh RS**, **Saini GK**, **Kennedy JF**. 2010. Maltotriose syrup preparation from pullulan using pullulanase. Carbohydr Polym **80**:401–407.

10. **Duan X**, **Chen J**, **Wu J**. 2013. Improving the thermostability and catalytic efficiency of *Bacillus deramificans* pullulanase by site-directed mutagenesis. Appl Environ Microbiol **79**:4072–4077.

11. **Rajaei S**, **Heidari R**, **Zahiri HS**, **Sharifzadeh S**, **Torktaz I**, **Noghabi KA**. 2014. A novel cold-adapted pullulanase from *Exiguobacterium* sp. SH3: Production optimization, purification, and characterization. Starch - Stärke **66**:225–234.

12. **Bertoldo C**, **Duffner F**, **Jorgensen PL**, **Antranikian G**. 1999. Pullulanase type I from *Fervidobacterium pennavorans* Ven5: cloning , sequencing, and expression of the gene and biochemical characterization of the recombinant enzyme. Appl Environ Microbiol **65**:2084–2091.

13. **Liu J**, **Liu Y**, **Yan F**, **Jiang Z**, **Yang S**, **Yan Q**. 2016. Gene cloning, functional expression and characterisation of a novel type I pullulanase from *Paenibacillus barengoltzii* and its application in resistant starch production. Protein Expr Purif **121**:22–30.

14. **Wei W**, **Ma J**, **Chen S-Q**, **Cai X-H**, **Wei D-Z**. 2015. A novel cold-adapted type I pullulanase of *Paenibacillus polymyxa* Nws-pp2: in vivo functional expression and biochemical characterization of glucans hydrolyzates analysis. BMC Biotechnol **15**:1–13.

15. **Wei W**, **Ma J**, **Guo S**, **Wei DZ**. 2014. A type I pullulanase of *Bacillus cereus* Nws-bc5 screening from

stinky tofu brine: Functional expression in *Escherichia coli* and *Bacillus subtilis* and enzyme characterization. Process Biochem **49**:1893–1902.

16. **Yang S**, **Yan Q**, **Bao Q**, **Liu J**, **Jiang Z**. 2016. Expression and biochemical characterization of a novel type I pullulanase from *Bacillus megaterium*. Biotechnol Lett.

17. **Chang M**, **Chu X**, **Lv J**, **Li Q**, **Tian J**, **Wu N**. 2016. Improving the thermostability of acidic pullulanase from *Bacillus naganoensis* by rational design. PLoS One **11**:e0165006.

18. **Kunamneni A**, **Singh S**. 2006. Improved high thermal stability of pullulanase from a newly isolated thermophilic *Bacillus* sp. AN-7. Enzyme Microb Technol **39**:1399–1404.

19. **Kim C-H**, **Choi H-I**, **Lee D-S**. 1993. Purification and biochemical properties of an alkaline pullulanase from alkalophilic *Bacillus* sp. S-1. Biosci Biotechnol Biochem **57**:1632–1637.

20. **Saha BC**, **Mathupala SP**, **Zeikus JG**. 1988. Purification and characterization of a highly thermostable novel pullulanase from *Clostridium thermohydrosulfuricum*. Biochem J **252**:343–348.

21. **Qiao Y**, **Peng Q**, **Yan J**, **Wang H**, **Ding H**, **Shi B**. 2015. Gene cloning and enzymatic characterization of alkali-tolerant type I pullulanase from *Exiguobacterium acetylicum*. Lett Appl Microbiol **60**:52–59.

22. **Waśko A**, **Polak-Berecka M**, **Targonski Z**. 2011. Purification and characterization of pullulanase from *Lactococcus lactis*. Prep Biochem Biotechnol **41**:252–261.

23. **Dunn G**, **Manners DJ**. 1975. The limit dextrinases from ungerminated oats (*Avena sativa* L) and ungerminated rice (*Oryza sativa* L). Carbohydr Res **39**:283–293.

24. **Hardie DG**, **Manners DJ**, **Yellowlees D**. 1976. The limit dextrinase from malted sorghum (*Sorghum vulgare*). Enzyme **50**:75–85.

25. **Masuda H**, **Takahashi T**, **Sugawara S**. 1987. Purification and properties of starch hydrolyzing enzymes in mature roots of sugar beets. Plant Physiol **84**:361–365.

26. **Kim CH**, **Nashiru O**, **Ko JH**. 1996. Purification and biochemical characterization of pullulanase type I from *Thermus caldophilus* GK-24. FEMS Microbiol Lett **138**:147–152.

27. **Møller MS**, **Windahl MS**, **Sim L**, **Bøjstrup M**, **Abou Hachem M**, **Hindsgaul O**, **Palcic M**, **Svensson B**, **Henriksen A**. 2015. Oligosaccharide and substrate binding in the starch debranching enzyme barley limit dextrinase. J Mol Biol **427**:1263–1277.

28. **Gordon RW**, **Manners DJ**, **Stark JR**. 1975. The limit dextrinase of the broad bean (*Vicia faba* L). Carbohydr Res **42**:125–134.